Pregnane X Receptor Deletion Modifies Recognition Memory and Electroencephalographic Activity

Badreddine Boussadia[a], **Laila Lakhal**[c], **Laurence Payrastre**[c], **Chaitali Ghosh**[e], **Jean-Marc Pascussi**[d], **Giuseppe Gangarossa**[#b,*], and **Nicola Marchi**[#a,*]

[a]Laboratory of Cerebrovascular Mechanisms of Brain Disorders, Department of Neuroscience, Institute of Functional Genomics, (UMR 5203 CNRS – U 1191 INSERM – Univ. Montpellier) Montpellier, France

[b]Université Paris Diderot, Sorbonne Paris Cité, Unité de Biologie Fonctionnelle et Adaptative (BFA), CNRS UMR 8251, F-75205 Paris, France

[c]Toxalim (Research Centre in Food Toxicology), Université de Toulouse, INRA, ENVT, INP-Purpan, UPS, Toulouse, France

[d]Laboratory Signalization, Plasticity and Cancer, Department of Cancer Biology, Institute of Functional Genomics, Montpellier, France

[e]Cerebrovascular Research, LRI Cleveland Clinic, USA

[#] These authors contributed equally to this work.

Abstract

Nuclear receptors (NR) are emerging as key players in the central nervous system (CNS) with reported implications in physiological and pathophysiological conditions. While a number of NR has been studied, it is unknown whether invalidation of the pregnane xenobiotic receptor (PXR, NR1I2) corresponds to neurological modifications in the adult brain. PXR$^{-/-}$ C57BL/6 J and wild-type mice were used to investigate: (*i*) recognition memory, motor coordination, and anxiety-like behaviors; (*ii*) longitudinal video-electroencephalographic (EEG) recordings and frequency wave analysis; (*iii*) neurovascular structures by histological evaluation and expression of the cerebrovascular tight junctions ZO1 and CLDN5. Absence of PXR was associated with anxiety-like behavior and recognition memory impairment in adult mice. The latter was simultaneous to an EEG signature of lower theta frequency during sleep and abnormal delta waves. Neurophysiological changes did not correspond to significant structural changes in the adult brain, expect for a localized and minor increase in the fronto-parietal neurovascular density and reduced ZO1, but not CLDN5, expression in isolated brain capillaries. Our results converge with existing evidence supporting a link between NR expression and brain physiology. Although the exact modalities remain to be elucidated, the possibility that extra-physiological modulation of PXR may constitute a pathophysiological entry point or a molecular target for brain diseases is proposed.

*Corresponding authors: giuseppe.gangarossa@univ-paris-diderot.fr(G. Gangarossa), nicola.marchi@igf.cnrs.fr (N. Marchi).

Keywords

nuclear receptor PXR; anxiety; recognition memory; EEG; neurovascular structure

INTRODUCTION

Nuclear receptors (NR) are transcription factors expressed in peripheral organs and have recently been studied in the brain (Bauer et al., 2004, 2006; Lamba et al., 2004; Marini et al., 2007; Mellon et al., 2008; Frye et al., 2011). Increasing experimental evidence supports a direct and indirect interplay between NR modulation and neuronal functions, including learning, memory, (Hawk et al., 2012; Yang and Wang, 2014; Kaur and Sodhi, 2015; Boussadia et al., 2016) and mood (Fan et al., 2008; Tan et al., 2012). In particular, the pregnane $\times$ receptor (PXR), a member of the NR1I sub-family, is involved in the metabolism or biotransformation of neurosteroids in the brain, possibly impacting behavior or neuronal plasticity (Frye et al., 2011, 2013). Further extending the role of NR is recent evidence indicating a link between their expression and developmental brain defects, organs' homeostasis and inflammatory processes (Xu et al., 2005; Ma et al., 2008; Ott et al., 2009; Venkatesh et al., 2014; Wang et al., 2014).

Despite this evidence, the link between PXR expression and brain functions remains to be fully clarified. We tested the hypothesis that genetic deletion of PXR may impact adulthood neurophysiological parameters. We now wish to provide proof-of-principle results pertinent to conditions where PXR is modified (e.g., loss of function) or inhibited. We performed an initial investigation using PXR knock-out mice studying possible modifications of spontaneous behaviors (anxiety, locomotion), recognition memory and motor learning. In addition, we executed a longitudinal video-electroencephalographic (EEG) monitoring to profile and measure brain wave oscillations which could parallel behavioral alterations. Considering that deletion of specific NR was reported to impact barriers and cortical neuronal structures (Fan et al., 2008; Tan et al., 2010; Venkatesh et al., 2014), we performed a histological investigation to determine whether a developmental brain phenotype is linked to PXR deletion.

EXPERIMENTAL PROCEDURES

Animals

All experiments followed European Union (Council directive 86/609EEC) and institutional guidelines of laboratory animals' usage. Mice were generated and genotyped at INRA-Toxalim animal facilities (institutional license approved by the French Ministry of Agriculture N° D34–172–13 and B31–555013). Mice were housed on a 12-h light/dark cycle with food and water ad *libitum*. Animal protocols were approved by the local ethics committee for animal testing (05185.01 and 00846.01). PXR$^{-/-}$ mice and wild type on a C57BL/6 J genetic background were originally established and previously used by the authors of this manuscript (INRA-Toxalim, as part of multiple colonies of NR KO mice (Marmugi et al., 2016). Colony founders were provided by Pr. Urs A Meyer (Biozentrum, University of Basel, Switzerland).

Behavioral studies

A total of $n = 11$ PXR$^{-/-}$ and $n = 11$ WT male mice (8–12 weeks) were used for behavioral testing. *Novel Place and Novel Object Recognition*. Recognition memory tests were performed as previously described (Gangarossa et al., 2014b,a). Briefly, after 10 min of habituation to the V-maze (novel object recognition, (Busquets-Garcia et al., 2013) or an arena (spatial object recognition), mice were allowed to explore two objects (Lego® of different colors and shapes). The object discrimination task started 24 h after habituation. During novel object recognition test one of the two objects was replaced by a new one while in the object-place recognition test one of the two objects was relocated within the arena. The time spent interacting with an object was recorded during the acquisition and retention periods. The experiments were videotaped and the time spent exploring the objects was scored. Interaction was defined as paws or mouse snout touching the object (distance less than 1 cm). The percentage of exploration was calculated as: $T_{new}/(T_{new} + T_{old}) \times 100$. *Rotarod test*. Balance and motor coordination as well as motor learning were assessed using a mouse accelerating rotarod (Ugo Basile, Comerio, Italy) as previously described (Gangarossa et al., 2014b,a). Briefly, mice were placed on the rotating drum accelerating from 4 to 40 rpm over 5 min, performing three trials a day for three consecutive days. The interval between trials was 45 min. We determined latency scores to fall or ride around the rod. *Spontaneous locomotor activity*. Locomotor activity was measured as previously described (Gangarossa et al., 2014b,a). Horizontal and vertical activities were determined in a circular corridor (Imetronic, Pessac, France). Counts for horizontal activity were defined as the interruption of two adjacent photobeams (placed at a height of 1 cm) within a 90° sector of the corridor and counts for vertical activity (rearing) as interruption of beams placed at a height of 7.5 cm along the corridor (mice stretching upwards) (Valjent et al., 2010). *Elevated-Plus Maze (EPM)*. The elevated plus maze (1 m above the floor) consisted of a black plastic structure with two open (5 cm width $\times$ 35 cm length $\times$ 0.5 cm height of the walls) and two closed arms (5 cm width $\times$ 35 cm length $\times$ 15 cm height of the walls). Mice were placed in the center of the maze facing one of the open arms and were allowed to explore for 10 min. Experiments were videotaped and scored for entries and time spent in the closed or open arms (four paws). *Open field*. Spontaneous exploratory behavior was monitored in an open field (white plastic arena; 35 cm width $\times$ 50 cm length $\times$ 20 cm height) for 10 min. The center zone was defined as a virtual perimeter within 5 cm from the sides of the arena. Experiments were videotaped and an observer scored the time spent in the center (four paws inside the center zone) and the number of transitions into the center zone.

Video-encephalography monitoring and signal analysis

Following anesthesia (ketamine/xylazine) mice were placed on a stereotaxic frame and the skull surgically exposed. A preamplifier (Pinnacle Inc., USA) was connected to fronto-parietal screw microelectrodes. Mice were allowed to recover one week after the surgery. Mice ($n = 4$ PXR$^{-/-}$ and $n = 4$ WT) were monitored using video-EEG (50 h/each; 50% night and 50% day) for one week. EEG signals were acquired at 200–600 Hz using a band pass filter (50–100 Hz) and analyzed using Neuroscore or MatLab. EEG samples (10 min each) were extracted from the recordings, distinguishing between: (i) light vs. dark phases; (ii) awake/exploratory vs. sleep. Video analysis ruled out EEG motion artifacts (eating, drinking or chewing), see (Boussadia et al., 2016). The following EEG portions were analyzed: $n =$

40 WT awake/exploratory, $n = 42$ WT sleep, $n = 32$ PXR$^{-/-}$ awake/exploratory and $n = 35$ PXR$^{-/-}$ sleep. Total EEG time analyzed was: 400 min for WT awake/exploratory, 420 min for WT sleep, 320 min for PXR$^{-/-}$ awake/exploratory and 350 min for PXR$^{-/-}$ sleep. EEG extracts were analyzed using Neuroscore (Periodogram Power Bands) and the relative abundance (0–100%) of each 0.5-Hz increment (0.5–30 Hz) was determined.

Microvessels isolation, immunohistochemistry and western blot

Capillary isolation: See also (Boussadia et al., 2016). Cortical and hippocampal microvessel samples were obtained in two separate experiments and pulled together from the following number of mice: experiment (*i*) $n = 5$ PXR$^{-/-}$ and $n = 5$ WT; experiment (*ii*) $n = 6$ PXR$^{-/-}$ and $n = 6$ WT. Briefly, white matter, meninges and midbrain were removed and the remaining tissue homogenized at 4°C. A 1:1 30% Ficoll:brain homogenate was centrifuged (5800g for 20 min). Capillaries were separated by filtration (>20 μm and <100 μm). *Western Blots*. Samples were separated by electrophoresis and transferred onto a nitro-cellulose membrane. Incubation with primary antibodies was performed overnight (4 °C) using mouse anti-Zona Occludens 1 (2 μg/ml, 1:400; 339100, Invitrogen, Paris, France), mouse anti-Claudin 5 (1 μg/ml, 1:800; 352500, Invitrogen, Paris, France) or mouse anti-Actin (1:10,000; ab6276, Abcam, Paris, France). Secondary antibody was a goat anti-mouse horseradish peroxidase (HRP)-conjugated (1:4000). Each WB band represents $n = 5$ and $n = 6$ mice. Similar protocol and identical antibodies were used for whole-brain tissue homogenates (hippocampi and cortices). WB quantification was performed using Fuji (densitometry).

Immunohistochemistry

Under anesthesia mice ($n = 4$ PXR$^{-/-}$ and $n = 4$ WT) were injected intracardially with 300 μL of a FITC-Albumin solution (25 mg/ml in PBS; Sigma-Aldrich). Brains were rapidly removed, post-fixed using 4% PFA (48 h) and coronal sections (30 μm) obtained using a vibratome. FITC$^+$ vessel quantification (length and number; Fiji skeleton Plug-in) was performed using 10× images ($n = 6$–10/each) of cortical structures (parietal and temporal), see also (Boussadia et al., 2016). Neurons were stained using a NeuN primary antibody (1:300; Millipore, MAB377, Fontenay sous Bois, France). Cortical thickness is the distance calculated (at least two measurements of 10× -captured images per sample) between the most external NeuN$^+$ cortical cell layer and the white matter border (Fiji). CA hippocampal thickness was similarly determined.

Statistics

Student's *t*-test with equal variances was used for groups of two, when applicable. Data were analyzed using a oneway ANOVA followed by Bonferroni post hoc test for specific comparisons. In all cases, significance threshold was set at $p < 0.05$. Statistical analyses were performed using GraphPad Prism 6.0 (GraphPad Prism Software Inc., San Diego, USA) or Origin Microcal.

RESULTS

Anxiety-like behavior and impaired recognition memory in PXR$^{-/-}$ mice

PXR$^{-/-}$ adult mice spent less time in the EPM open arms as compared to WT mice (Fig. 1A). In addition, the number of entries into the open and closed arms was significantly reduced in PXR$^{-/-}$ mice (Fig. 1B, C). This abnormal spontaneous phenotype was confirmed using the open field test (OF, novel and stressful environment). PXR$^{-/-}$ mice spent less time in the center of the arena (Fig. 1D), also performing fewer transitions as compared to WT mice (Fig. 1E). Importantly, spontaneous locomotor activity was similar between PXR$^{-/-}$ and WT mice, ruling out the possibility that behavioral changes could derive from defects in locomotion. No differences were measured in spontaneous horizontal (Fig. 1F, G) or vertical activities (Fig. 1H, I), indicating intact exploratory drive.

The novel place (NPR, Fig. 2A) and the novel object recognition (NOR, Fig. 2D) were then performed to determine memory functions (Fig. 2). PXR$^{-/-}$ mice did not show a preference for familiar or relocated objects during the recall session of the NPR test (24 h after the exploration phase), as compared to WT mice (Fig. 2B,C). The latter result was not due to an impairment of the exploratory drive as the cumulative time of objects' exploration did not change during the familiarization or recall phase (*data not shown*). During the NOR test (Fig. 2D) PXR$^{-/-}$ mice did not prefer the familiar vs. the relocated object throughout the recall session, indicating reduced recognition memory functions (Fig. 2E, F). This phenotype was not due to impaired spontaneous exploratory drive or altered locomotor activity (see Fig. 1).

Procedural motor learning (accelerating Rotarod test) was performed to determine whether the dysfunctions observed in PXR$^{-/-}$ mice were generalized to other forms of learning and memory processes. No differences were observed during the first day of training, suggesting unaltered motor functions and coordination in PXR$^{-/-}$ mice (Fig. 2G). In addition, PXR$^{-/-}$ mice showed normal improvements of motor performance during consecutive training sessions (Fig. 2G), comparable to WT mice and suggesting intact motor learning ability. Taken together, our results indicate that genetic ablation of PXR negatively impacts recognition memory and learning performances, sparing locomotor coordination, spontaneous activity, and procedural motor learning. These results converge with previous reports indicating a potential link between NR expression and brain functions (Fan et al., 2008; Tan et al., 2010, 2012; Boussadia et al., 2016).

Basal *in vivo* electrographic signature of PXR$^{-/-}$ mice

The characterization of the basal EEG activity *in vivo* is often used to substantiate behavioral investigations (Seager et al., 2002; Buzsaki, 2005; Sauseng et al., 2010). To this end, EEG signals were analyzed in PXR$^{-/-}$ and WT mice during awake/exploratory and sleep periods. PXR$^{-/-}$ mice displayed a decrease in 5–10-Hz EEG waves during sleep, suggesting impaired theta rhythm (Fig. 3A), while no significant differences were quantified during awake periods (Fig. 3A1). Interestingly, EEG cortical activity between 0.5 and 4 Hz (delta) was increased in PXR$^{-/-}$ mice during both awake/exploratory and sleep phases. Changes in theta and delta waves were previously suggested to be associated with memory

defects (Vakalopoulos, 2014). Importantly, the profile of EEG waves >20 Hz was identical between PXR$^{-/-}$ and WT mice, indicating specificity of the changes reported at lower frequencies (Fig. 3B, B1). Examples of time-joint frequency analysis corresponding to decreased theta during sleep and increased delta in PXR$^{-/-}$ mice are shown in Fig. 3C1–D1.

Lack of important neuro-vascular structural modifications in PXR$^{-/-}$ mice

Previous reports showed modification of neuronal cortical structures in animals where specific NR were genetically deleted, introducing a possible role for NR in brain development (Fan et al., 2008; Tan et al., 2010, 2012). Therefore, we examined whether neurophysiological changes in PXR$^{-/-}$ adult mice are associated with neuronal and vascular modifications. In general, structural defects were not observed, except for a localized increase in NeuN^{+} neurons density (Fig. 4A, C, D) and FITC^{+} microvessels length (Fig. 4B, E) in the fronto-parietal cortices. No significant morphological changes were detected in the hippocampus (Fig. 4C, D).

A reduction of tight junction (TJ) proteins expression has been observed in peripheral barriers in PXR$^{-/-}$ mice (Venkatesh et al., 2014). We therefore analyzed the expression of two main TJ proteins, ZO1 and CLDN5, at the blood–brain barrier. We found a significant decrease of the TJ protein ZO1 in the cortex and in cortical microvessels isolated from PXR$^{-/-}$ mice (Fig. 4F, H). However, CLDN5 expression was unchanged (Fig. 4G, I, J). Taken together, these results exclude a significant structural phenotype (e.g., neurovascular malformations or ectopias) resulting from PXR deletion. Nevertheless, reduced TJ proteins may support a mechanism of homeostatic brain changes, also consistent with previously published reports (Venkatesh et al., 2014).

DISCUSSION

Our results converge with existing evidence supporting the contribution of NR to neuronal physiology. We found that absence of PXR is associated with anxiety-like behavior, recognition memory impairments, and a specific cortical EEG signature, e.g., lower theta frequency during sleep and abnormal delta frequency. Existing evidence points to brain developmental changes associated with loss of specific NR (Fan et al., 2008; Tan et al., 2010, 2012; Venkatesh et al., 2014). Our results do not support a major role of PXR in the development of brain neuro-vascular structures. Instead, they are consistent with a potential link between PXR and the metabolism of endogenous molecules (Tolson and Wang, 2010). In this respect, PXR antisense oligonucleotide infused in the ventral tegmental area was shown to alter brain levels of 3α,5α-THP and to induce behavioral changes (Frye et al., 2011, 2013, 2014). PXR expression in the midbrain is responsible for aspects of social behavior (Frye et al., 2014). In addition, the PXR agonist rifampicin (Chen and Raymond, 2006) reduced memory deficits, an effect that was reversed when the PXR antagonist ketoconazole (Duret et al., 2006) was co-administered (Kaur and Sodhi, 2015). These observations are consistent with the hypothesis that PXR may control biotransformation routes in the brain, e.g., possibly impacting the metabolism of neuronal acting molecules (Frye et al., 2011).

In the present study, a battery of behavioral tests was complemented by EEG recordings of basal neuronal activity. Specific EEG read-outs can be used as an index of perceptual, sensorimotor, cognitive processes (Duzel et al., 2010) and of neuromodulation in memory disorders (Vakalopoulos, 2014). For instance, behavioral spatial deficits correlate with decreased theta oscillations in rodents (Chauviere et al., 2009) while increased efficiency of memory encoding was shown during periods of high theta amplitude (Seager et al., 2002; Buzsaki, 2005; Sauseng et al., 2010). Reduction of theta waves during sleep has been recorded in mouse models of Alzheimer's disease (AD) (Scott et al., 2012; Schneider et al., 2014). Although less studied, delta oscillations have been related to cognitive processing (Knyazev, 2012; Harmony, 2013) while increased delta waves have been observed in AD patients (van der Hiele et al., 2007; Moretti et al., 2010) as well as AD mice (Schneider et al., 2014). Even though, in our model, a casual-relationship between altered EEG and behavioral impairments may exist, the results presented herein do not allow such a conclusion to be drawn. We cannot fully exclude the possibility that genetic ablation of PXR could have resulted in molecular adaptations responsible for behavioral impairments (Bailey et al., 2006). However, the specificity of the behavioral readouts (e.g. impaired recognition memory, increased anxiety, intact motor learning and locomotor activity) supports our experimental conclusions.

Developmental vs. adult NR expression and function

Our results do not indicate substantial modifications of the neurovascular architecture in adult PXR$^{-/-}$ mice. Although statistically significant, the observed increase in neurovascular density may be insufficient to underscore a neurophysiological phenotype. We nevertheless speculate that a reduced expression of selected cerebrovascular TJ proteins, as found in adult PXR$^{-/-}$ mice, could favor an increase of endothelial permeability, perhaps engaging angiogenic signals. Previous evidence supports cerebrovascular permeability as a mechanism of neuronal hyper-excitability. Vascular permeability topographically overlaps with electrographic pathological changes (Friedman, 2011; Friedman and Kaufer, 2011; Marchi et al., 2012). Whether the above-described evidence applies to our experimental model remains to be assessed. Other NR have been found to impact developmental stages as indicated by neuro-glial modifications in LXR$^{-/-}$ mice (Fan et al., 2008). Furthermore, absence of the PXR cognate receptor CAR was associated with discrete signs of neuro-vascular inflammation in the adult mouse brain (Boussadia et al., 2016).

CONCLUSIONS

PXR is expressed in peripheral organs (liver, guts) and in the CNS. The extra-physiological modulation (e.g., inhibition) of PXR can occur during exposure to xenobiotics or to environmental contaminants, impacting the expression of downstream targets, such as cytochrome metabolic enzymes (Graillot et al., 2012). The dysregulation of cytochrome enzymes can, in turn, modify the pharmacokinetic profiles and the effects of endogenous molecules, in the brain and/or the periphery. The latter is relevant to public health as metabolic diseases can affect neurological functions. Completing the loop are clinical and experimental evidence of blood-brain barrier permeability as a pathophysiological

contributor to seizures, cognitive impairments, and vascular dementia (Friedman and Kaufer, 2011).

The increasing attention to NR, and more specifically to NR1I xenoreceptors, is justified by their involvement in an expanding array of cellular functions. In summary, neurovascular physiology may depend, at least in part, on NR modulation, the latter potentially impacting the biotransformation of endogenous or exogenous molecules.

Acknowledgments—

Abbreviations:

AD	Alzheimer's disease
EEG	electroencephalographic
EPM	Elevated-Plus Maze
NPR	novel place recognition
NR	Nuclear receptor
PXR	pregnane xenobiotic receptor
TJ	tight junction

REFERENCES

Bailey KR, Rustay NR, Crawley JN (2006) Behavioral phenotyping of transgenic and knockout mice: practical concerns and potential pitfalls. ILAR J 47:124–131. [PubMed: 16547369]

Bauer B, Hartz AM, Fricker G, Miller DS (2004) Pregnane × receptor up-regulation of P-glycoprotein expression and transport function at the blood-brain barrier. Mol Pharmacol 66:413–419. [PubMed: 15322232]

Bauer B, Yang X, Hartz AM, Olson ER, Zhao R, Kalvass JC, Pollack GM, Miller DS (2006) In vivo activation of human pregnane × receptor tightens the blood–brain barrier to methadone through P-glycoprotein up-regulation. Mol Pharmacol 70:1212–1219. [PubMed: 16837625]

Boussadia B, Gangarossa G, Mselli-Lakhal L, Rousset MC, de Bock F, Lassere F, Ghosh C, Pascussi JM, Janigro D, Marchi N (2016) Lack of CAR impacts neuronal function and cerebrovascular integrity in vivo. Exp Neurol 283:39–48. [PubMed: 27240521]

Busquets-Garcia A, Gomis-Gonzalez M, Guegan T, Agustin-Pavon C, Pastor A, Mato S, Perez-Samartin A, Matute C, de la Torre R, Dierssen M, Maldonado R, Ozaita A (2013) Targeting the endocannabinoid system in the treatment of fragile × syndrome. Nat Med 19:603–607. [PubMed: 23542787]

Buzsaki G (2005) Theta rhythm of navigation: link between path integration and landmark navigation, episodic and semantic memory. Hippocampus 15:827–840. [PubMed: 16149082]

Chauviere L, Rafrafi N, Thinus-Blanc C, Bartolomei F, Esclapez M, Bernard C (2009) Early deficits in spatial memory and theta rhythm in experimental temporal lobe epilepsy. J Neurosci 29:5402–5410. [PubMed: 19403808]

Chen J, Raymond K (2006) Roles of rifampicin in drug-drug interactions: underlying molecular mechanisms involving the nuclear pregnane × receptor. Ann Clin Microbiol Antimicrob 5:3. [PubMed: 16480505]

Duret C, Daujat-Chavanieu M, Pascussi JM, Pichard-Garcia L, Balaguer P, Fabre JM, Vilarem MJ, Maurel P, Gerbal-Chaloin S (2006) Ketoconazole and miconazole are antagonists of the human glucocorticoid receptor: consequences on the expression and function of the constitutive androstane receptor and the pregnane × receptor. Mol Pharmacol 70:329–339. [PubMed: 16608920]

Duzel E, Penny WD, Burgess N (2010) Brain oscillations and memory. Curr Opin Neurobiol 20:143–149. [PubMed: 20181475]

Fan X, Kim HJ, Bouton D, Warner M, Gustafsson JA (2008) Expression of liver × receptor beta is essential for formation of superficial cortical layers and migration of later-born neurons. Proc Natl Acad Sci U S A 105:13445–13450. [PubMed: 18768805]

Friedman A (2011) Blood-brain barrier dysfunction, status epilepticus, seizures, and epilepsy: a puzzle of a chicken and egg? Epilepsia 52(Suppl 8):19–20. [PubMed: 21967353]

Friedman A, Kaufer D (2011) Blood-brain barrier breakdown and blood-brain communication in neurological and psychiatric diseases. Cardiovasc Psychiatry Neurol 2011:431470. [PubMed: 21747970]

Frye CA, Paris JJ, Walf AA, Rusconi JC (2011) Effects and mechanisms of 3α,5α,-THP on emotion, motivation, and reward functions involving pregnane xenobiotic receptor. Front Neurosci 5:136. [PubMed: 22294977]

Frye CA, Koonce CJ, Walf AA (2013) Pregnane xenobiotic receptors and membrane progestin receptors: role in neurosteroid-mediated motivated behaviours. J Neuroendocrinol 25:1002–1011. [PubMed: 24028379]

Frye CA, Koonce CJ, Walf AA (2014) The pregnane xenobiotic receptor, a prominent liver factor, has actions in the midbrain for neurosteroid synthesis and behavioral/neural plasticity of female rats. Front Syst Neurosci 8:60. [PubMed: 24795576]

Gangarossa G, Ceolin L, Paucard A, Lerner-Natoli M, Perroy J, Fagni L, Valjent E (2014a) Repeated stimulation of dopamine D1-like receptor and hyperactivation of mTOR signaling lead to generalized seizures, altered dentate gyrus plasticity, and memory deficits. Hippocampus 24:1466–1481. [PubMed: 25044816]

Gangarossa G, Laffray S, Bourinet E, Valjent E (2014b) T-type calcium channel Cav3.2 deficient mice show elevated anxiety, impaired memory and reduced sensitivity to psychostimulants. Front Behav Neurosci 8:92. [PubMed: 24672455]

Graillot V, Takakura N, Hegarat LL, Fessard V, Audebert M, Cravedi JP (2012) Genotoxicity of pesticide mixtures present in the diet of the French population. Environ Mol Mutagen 53:173–184. [PubMed: 22389207]

Harmony T (2013) The functional significance of delta oscillations in cognitive processing. Front Integr Neurosci 7:83. [PubMed: 24367301]

Hawk JD, Bookout AL, Poplawski SG, Bridi M, Rao AJ, Sulewski ME, Kroener BT, Manglesdorf DJ, Abel T (2012) NR4A nuclear receptors support memory enhancement by histone deacetylase inhibitors. J Clin Investig 122:3593–3602. [PubMed: 22996661]

Kaur P, Sodhi RK (2015) Memory recuperative potential of rifampicin in aluminum chloride-induced dementia: role of pregnane × receptors. Neuroscience 288:24–36. [PubMed: 25545714]

Knyazev GG (2012) EEG delta oscillations as a correlate of basic homeostatic and motivational processes. Neurosci Biobehav Rev 36:677–695. [PubMed: 22020231]

Lamba V, Yasuda K, Lamba JK, Assem M, Davila J, Strom S, Schuetz EG (2004) PXR (NR1I2): splice variants in human tissues, including brain, and identification of neurosteroids and nicotine as PXR activators. Toxicol Appl Pharmacol 199:251–265. [PubMed: 15364541]

Ma X, Idle JR, Gonzalez FJ (2008) The pregnane × receptor: from bench to bedside. Expert Opin Drug Metab Toxicol 4:895–908. [PubMed: 18624678]

Marchi N, Granata T, Ghosh C, Janigro D (2012) Blood-brain barrier dysfunction and epilepsy: pathophysiologic role and therapeutic approaches. Epilepsia 53:1877–1886. [PubMed: 22905812]

Marini S, Nannelli A, Sodini D, Dragoni S, Valoti M, Longo V, Gervasi PG (2007) Expression, microsomal and mitochondrial activities of cytochrome P450 enzymes in brain regions from control and phenobarbital-treated rabbits. Life Sci 80:910–917. [PubMed: 17161434]

Marmugi A, Lukowicz C, Lasserre F, Montagner A, Polizzi A, Ducheix S, Goron A, Gamet-Payrastre L, Gerbal-Chaloin S, Pascussi JM, Moldes M, Pineau T, Guillou H, Mselli-Lakhal L (2016) Activation of the constitutive androstane receptor induces hepatic lipogenesis and regulates Pnpla3 gene expression in a LXR-independent way. Toxicol Appl Pharmacol 303:90–100. [PubMed: 27180240]

Mellon SH, Gong W, Schonemann MD (2008) Endogenous and synthetic neurosteroids in treatment of niemann-pick type C disease. Brain Res Rev 57:410–420. [PubMed: 17629950]

Moretti DV, Pievani M, Geroldi C, Binetti G, Zanetti O, Rossini PM, Frisoni GB (2010) EEG markers discriminate among different subgroup of patients with mild cognitive impairment. Am J Alzheimers Dis Other Demen 25:58–73. [PubMed: 19204371]

Ott M, Fricker G, Bauer B (2009) Pregnane × receptor (PXR) regulates P-glycoprotein at the blood–brain barrier: functional similarities between pig and human PXR. J Pharmacol Exp Therap 329:141–149. [PubMed: 19147857]

Sauseng P, Griesmayr B, Freunberger R, Klimesch W (2010) Control mechanisms in working memory: a possible function of EEG theta oscillations. Neurosci Biobehav Rev 34:1015–1022. [PubMed: 20006645]

Schneider F, Baldauf K, Wetzel W, Reymann KG (2014) Behavioral and EEG changes in male 5×FAD mice. Physiol Behav 135:25–33. [PubMed: 24907698]

Scott L, Feng J, Kiss T, Needle E, Atchison K, Kawabe TT, Milici AJ, Hajos-Korcsok E, Riddell D, Hajos M (2012) Age-dependent disruption in hippocampal theta oscillation in amyloid-beta overproducing transgenic mice. Neurobiol Aging 33(1481): e1413–1423.

Seager MA, Johnson LD, Chabot ES, Asaka Y, Berry SD (2002) Oscillatory brain states and learning: Impact of hippocampal theta-contingent training. Proc Natl Acad Sci U S A 99:1616–1620. [PubMed: 11818559]

Tan XJ, Fan XT, Kim HJ, Butler R, Webb P, Warner M, Gustafsson JA (2010) Liver × receptor beta and thyroid hormone receptor alpha in brain cortical layering. Proc Natl Acad Sci U S A 107:12305–12310. [PubMed: 20566868]

Tan XJ, Dai YB, Wu WF, Warner M, Gustafsson JA (2012) Anxiety in liver × receptor beta knockout female mice with loss of glutamic acid decarboxylase in ventromedial prefrontal cortex. Proc Natl Acad Sci U S A 109:7493–7498. [PubMed: 22529354]

Tolson AH, Wang H (2010) Regulation of drug-metabolizing enzymes by xenobiotic receptors: PXR and CAR. Adv Drug Deliv Rev 62:1238–1249. [PubMed: 20727377]

Vakalopoulos C (2014) The EEG as an index of neuromodulator balance in memory and mental illness. Front Neurosci 8:63. [PubMed: 24782698]

Valjent E, Bertran-Gonzalez J, Aubier B, Greengard P, Herve D, Girault JA (2010) Mechanisms of locomotor sensitization to drugs of abuse in a two-injection protocol. Neuropsychopharmacology 35:401–415. [PubMed: 19759531]

van der Hiele K, Vein AA, van der Welle A, van der Grond J, Westendorp RG, Bollen EL, van Buchem MA, van Dijk JG, Middelkoop HA (2007) EEG and MRI correlates of mild cognitive impairment and Alzheimer's disease. Neurobiol Aging 28:1322–1329. [PubMed: 16854500]

Venkatesh M, Mukherjee S, Wang H, Li H, Sun K, Benechet AP, Qiu Z, Maher L, Redinbo MR, Phillips RS, Fleet JC, Kortagere S, Mukherjee P, Fasano A, Le Ven J, Nicholson JK, Dumas ME, Khanna KM, Mani S (2014) Symbiotic bacterial metabolites regulate gastrointestinal barrier function via the xenobiotic sensor PXR and Toll-like receptor 4. Immunity 41:296–310. [PubMed: 25065623]

Wang S, Lei T, Zhang K, Zhao W, Fang L, Lai B, Han J, Xiao L, Wang N (2014) Xenobiotic pregnane × receptor (PXR) regulates innate immunity via activation of NLRP3 inflammasome in vascular endothelial cells. J Biol Chem 289:30075–30081. [PubMed: 25202020]

Xu DX, Chen YH, Wang JP, Sun MF, Wang H, Wei LZ, Wei W (2005) Perinatal lipopolysaccharide exposure downregulates pregnane × receptor and Cyp3a11 expression in fetal mouse liver. Toxicol Sci 87:38–45. [PubMed: 15976188]
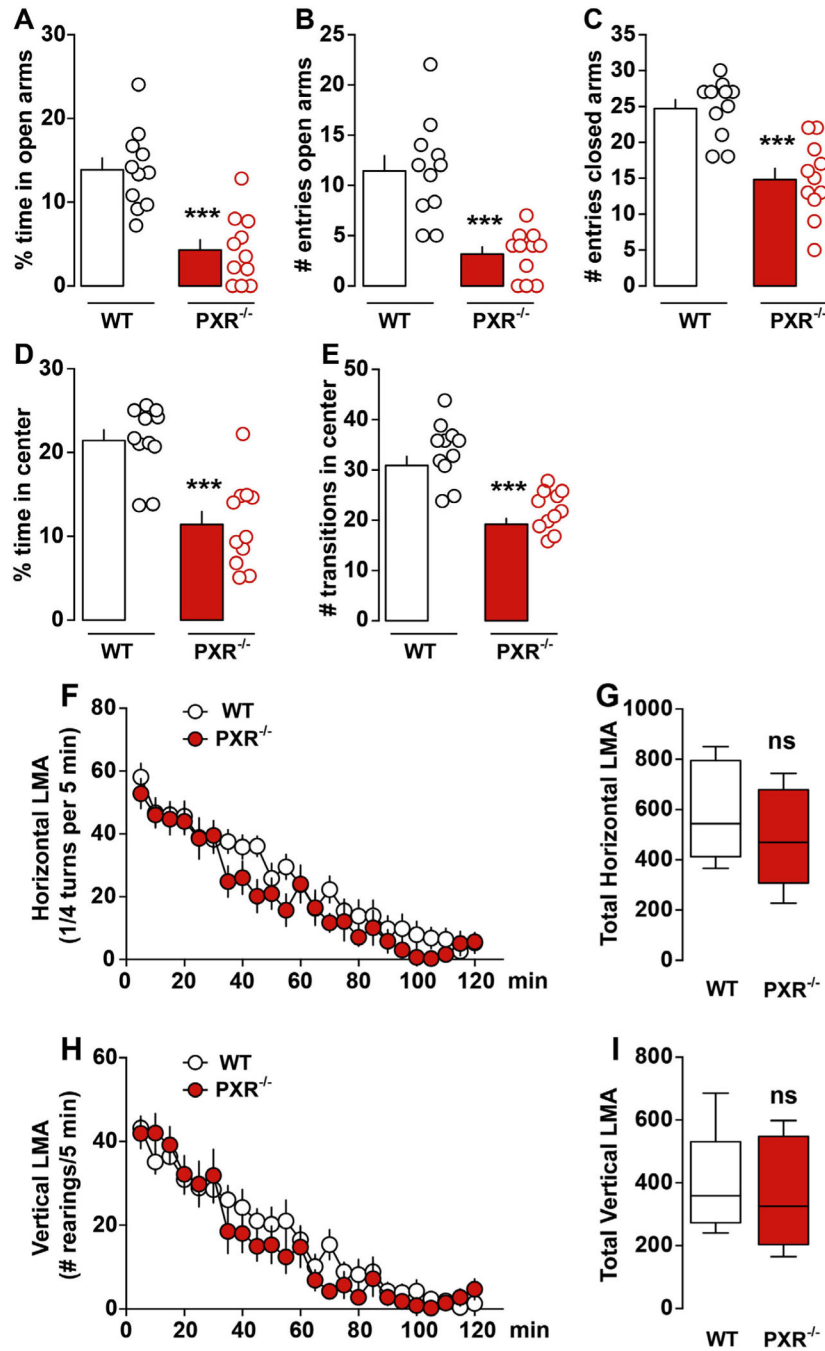
Yang H, Wang H (2014) Signaling control of the constitutive androstane receptor (CAR). Protein Cell 5:113–123. [PubMed: 24474196]

Fig. 1.

PXR$^{-/-}$ adult male mice show increased anxiety-like behavior but intact locomotor activity. (A) Time spent in the open arms during testing. (B-C) Number of entries in the open and closed arms ($n = 11$ mice each group). (D) Histograms show the percentage of time PXR$^{-/-}$ ($n = 11$) and WT mice ($n = 11$) spent in the center zone of the open field. (E) Histograms indicate the number of transitions PXR$^{-/-}$ ($n = 11$) and WT mice ($n = 11$) performed in the center zone of the open field. All data (mean ± SEM) were analyzed using Student's t-test: ***$p < 0.001$. (F) Spontaneous horizontal and (H) vertical (rearing) locomotor activity in

PXR$^{-/-}$ mice (novel non-stressful environment). Data were analyzed using a two-way ANOVA: (Time Genotype: $F_{(23,480)} = 0.68$, $P = 0.86$; Time: $F_{(23,480)} = 28.28$, $p < 0.0001$; Genotype: $F_{(1,480)} = 15.21$, $p < 0.0001$) (F). Two-way ANOVA: (Time × Genotype: $F_{(23,480)} = 0.81$, $P = 0.72$; Time: $F_{(23,480)} = 31.22$, $p < 0.0001$; Genotype: $F_{(1,480)} = 4.60$, $p < 0.0001$) (H). (G, I) Histograms show cumulative activities. Student's t-test: $p > 0.05$, ns.
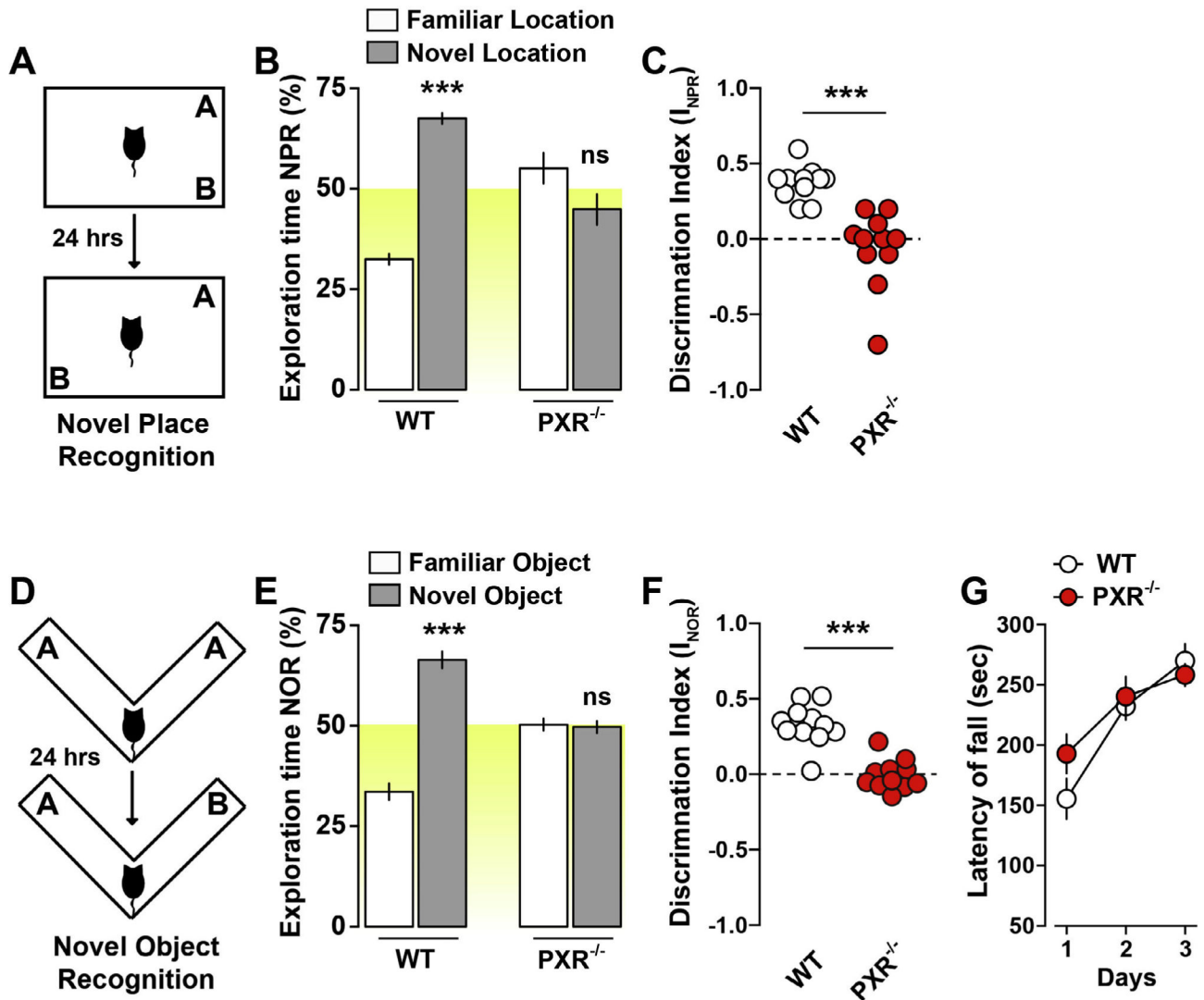
Fig. 2.
PXR$^{-/-}$ adult male mice show impaired recognition memory but intact coordination and motor learning. (A) Novel place recognition test. (B) Time of exploration of the novel location in PXR$^{-/-}$ mice. Data were analyzed using a two-way ANOVA: (Object exploration × Genotype: $F_{(1,40)} = 62.07$, $p < 0.0001$). Specific comparisons: ***$p < 0.001$ (WT-new *vs* WT-familiar). (C) Discrimination index in PXR$^{-/-}$ mice (novel place recognition test). Data (mean ± SEM) were analyzed using Student's *t*-test: ***$p < 0.001$. (D) Novel Object Recognition test. (E) Time of exploration of the novel object. Data were analyzed using a two-way ANOVA: (Object exploration × Genotype: $F_{(1,40)} = 86.40$, $p < 0.0001$). Specific comparisons: ***$p < 0.001$ (WT-new *vs* WT-familiar). (F) Discrimination index in PXR$^{-/-}$ mice (novel object recognition test). Data (mean ± SEM) were analyzed using Student's *t*-test: ***$p < 0.001$. (G) Coordination and motor learning over a training period of 3 days in PXR$^{-/-}$ mice (rotarod). Data were analyzed using a two-way ANOVA (Time × Genotype: $F_{(2,60)} = 1.48$, $P = 0.23$; Time: $F_{(2,60)} = 20.47$, $p < 0.0001$; Genotype: $F_{(1,60)} = 0.92$, $P = 0.34$). $n = 11$ mice per group were used.
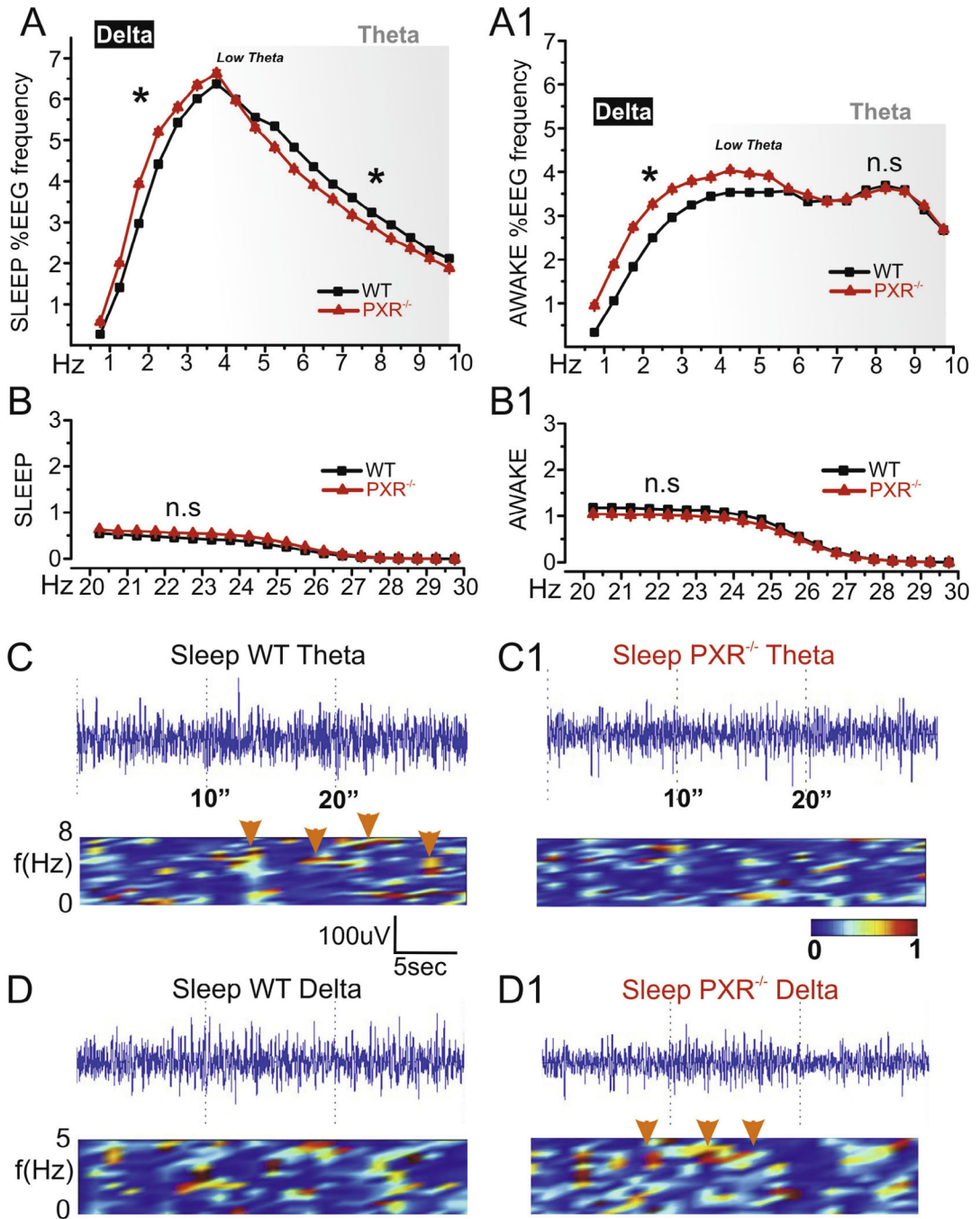
Fig. 3.

Electroencephalographic signature in adult PXR$^{-/-}$ mice. Each data point corresponds to a 0.5-Hz range, as indicated on the X axis. (A) During sleep periods PXR$^{-/-}$ mice displayed reduced 5–10-Hz EEG activity (theta waves, *gray shadow*). (A1) Theta frequency were similar between PXR$^{-/-}$ and WT mice during awake-exploration periods. Interestingly 0.5–4-Hz (delta) waves were generally increased in PXR$^{-/-}$ mice. (B, B1) No differences were measured at Hz > 20 (C–C1) Examples of EEG and time-joint frequency analysis showing
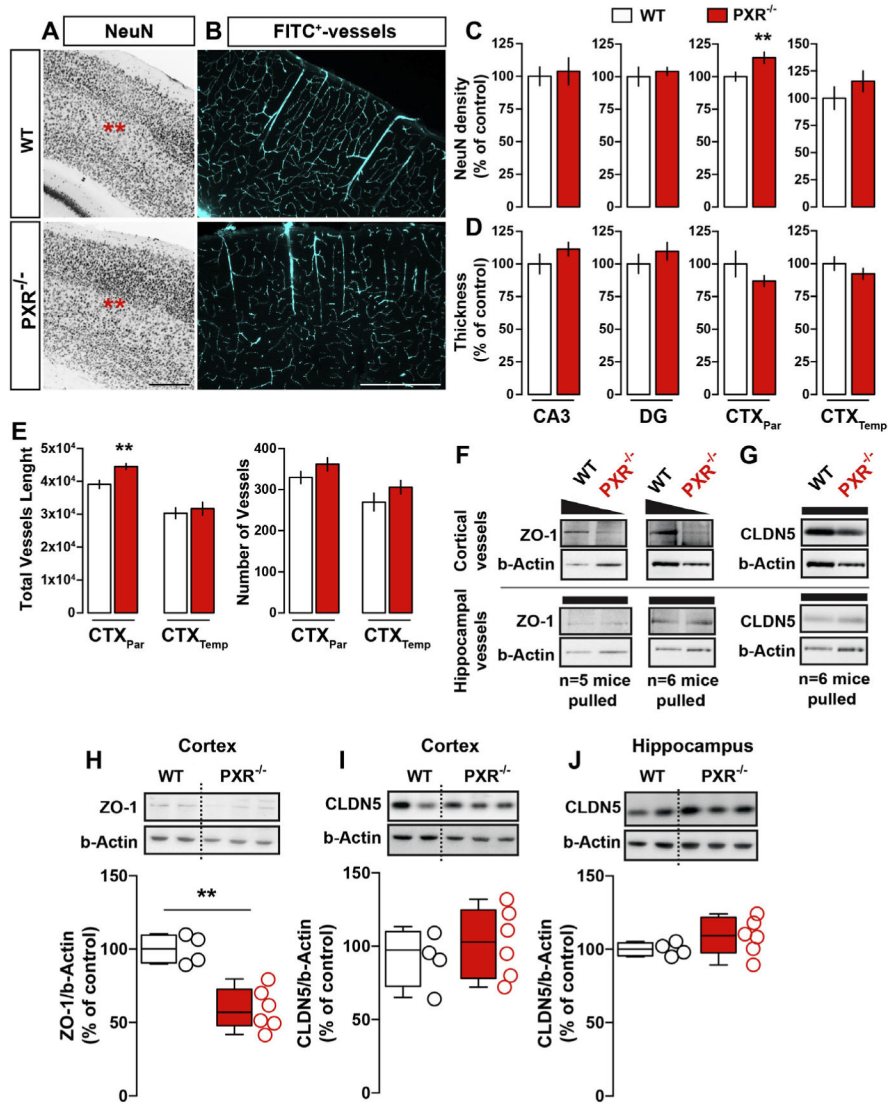
decreased theta in PXR$^{-/-}$ during sleep (*arrows*). (D–D1) Example of delta bands in PXR$^{-/-}$ mice.

Fig. 4.
Negligible structural neurovascular modifications in the adult PXR$^{-/-}$ brain. (A) Immunohistochemical detection of NeuN in the cortex of PXR$^{-/-}$ and WT mice. Scale bar = 1 mm. (B) Immunohistochemical reconstruction of FITC-positive vessels in the cortex. Scale bar = 1 mm. (C) Histograms show quantifications for NeuN density. Student's *t*-test: $p < 0.01$. (D) Histograms show thickness of hippocampal and cortical regions. (E) Histograms show quantifications of the total vessels length and the number of microvessels. Student's *t*-test: $^{**}p < 0.01$. (F) Detection of ZO1 and CLDN5 in purified cortical and hippocampal microvessels in two distinct set of experiments (5–6 mice per genotype are pulled together to obtain pure vessels fractions). Histograms show western blot quantifications of cortical ZO-1 (H), cortical (I) and hippocampal (J) CLDN5. Student's *t*-test: $^{**}p < 0.01$, $n = 4$–6 mice per group.